

International Conference on Concentrating Solar Power and Chemical Energy Systems,
SolarPACES 2014

Thermo-physical properties of a steel-making by-product to be used as thermal energy storage material in a packed-bed system

I. Ortega^a, A. Faik^{a, *}, A. Gil^a, J. Rodríguez-Aseguinolaza^a and B. D'Aguanno^a

^a*CIC Energigune, Albert Einstein 48, Miñano (Álava) 01510, Spain*

Abstract

In this paper the valorisation of an industrial and cheap by-product from the steel manufacturing, Electric Arc Furnace slag, is studied as new thermal energy storage material in a packed-bed system. For this application, the driving thermo-physical and the thermal and chemical stability of two different slags have been studied. The obtained results have revealed that this material presents similar properties to other materials typically studied as filler/thermal energy storage material in a packed-bed arrangement. The thermal stability and compatibility analysis have indicated that the slag is stable, at least up to 1000°C when working in direct contact with air as heat transfer fluid. In addition, in this work, a heat storage system based on air-packed bed configuration is proposed. In this frame, different operation methods have been computationally analysed in order to maximize the storage capacity and efficiency of the packed-bed design. Overall, this work has demonstrated the high potential of this waste material to obtain an efficient and cost-effective thermal energy storage solution.

© 2015 The Authors. Published by Elsevier Ltd. This is an open access article under the CC BY-NC-ND license (<http://creativecommons.org/licenses/by-nc-nd/4.0/>).

Peer review by the scientific conference committee of SolarPACES 2014 under responsibility of PSE AG

Keywords: concentrated solar power (CSP); electric arc furnace (EAF); thermal energy storage (TES); thermocline; slag; solid waste; ceramic.

1. Introduction

Thermal energy storage (TES) is a key issue in concentrated solar power (CSP) plants in order to increase the global efficiency of the electricity generation process. Current, TES technologies implemented in commercial plants are based on molten salts (usually so-called Solar Salt, a mixture of 60%_w NaNO₃ and 40%_w KNO₃) as sensible heat

* Corresponding author. Tel.: +34 945297108.
E-mail address: afaik@cicenergigune.com

storage material [1-2]. However, this storage material presents several limitations such as the operation temperature range, limited between 260-565 °C and a low thermal conductivity, which leads to complex heat exchanger systems. Next generation of power tower plants will need to overcome these limitations in order to allow higher operation temperatures (up to 800°C) and cost-effective thermal storage solutions. In this frame, SunShot Initiative, launched by US DoE, aims to reduce the total installed cost of solar energy systems to \$0.06 per kWh by 2020 [3]. Consequently, in order to meet this objective, alternative heat transfer fluids (HTF) and heat storage materials will have to be implemented.

One of the proposed strategies for the development of a cost-effective TES system is the substitution of the expensive solar salt by different low-cost materials [4, 5]. In addition, the implementation of a single storage tank instead the two tank design might also help to reduce the total storage system cost. In this context, packed-bed storage unit based on thermocline principle has revealed a high performance heat storage capability combined with the desired cost reduction.

A packed-bed storage system basically consists on a storage tank filled with different shape and size particles of a given solid material where the heat is loaded or removed by the circulation of a HTF through the free space between the filler particles. Singh et al. [6] presented a review on packed-bed systems with a list of potential filler materials and their corresponding thermo-physical properties. Between them, there are rocks, sand, bricks, metals and concrete. The selection of the best candidate, according to Khare et al. [7], should take into account not only the thermo-physical properties but also chemical properties (non-toxic, non-explosive, low corrosion potential, compatible with construction materials) as well as environmental and economic aspects (low manufacturing energy requirement and CO₂ footprint and widely available with a low cost).

In this frame, different authors focus their efforts on the characterization of different industrial waste materials in order to use them as sensible heat TES materials. Among them, Py et al. [8], studied a recycled industrial ceramic made by vitrification of asbestos containing wastes, also known as Cofalit[®]. This material was thermo-physically characterized by Faik et al. [9] and Calvet et al. [10], who also studied its compatibility with molten salts up to 500 °C [11] in order to use it in direct contact in packed-bed systems. On the other hand, fly-ashes were also suggested and studied by Meffre et al. [12]. Recently, Navarro et al. [13] characterized the thermal and mechanical properties of a by-product from pyrometallurgical refining process of copper and two by-products of the mineral industry of the potash production (one mainly containing silica oxide and the other one containing sodium chloride, respectively). The last by-product was even tested in a laboratory scale prototype [14] under different conditions of the material: as received and compacted, by adding the necessary proportion of water to the by-product.

In this work, steel slag, which is one of the main by-products of the steelmaking industry, is proposed as heat storage material. More than 1400 million tons of crude steel were produced worldwide in 2010 and EU contributed with almost 175 million tones. As a consequence, according to the European Slag Association around 45.3 million tons of ferrous slags were produced in Europe (23.5 million tones corresponding to blast furnace slag and 21.8 corresponding to electric arc furnace) [15]. From this amount, around 76% is reused on several applications such as road construction, cement production, hydraulic engineering and others. However, the other 24% is landfilled or stored in the steelmaker itself [15] which represents a huge potential of available material which might be enough to provide storage material for the CSP plants according to their announced growth previsions.

In this study, worldwide representative electric arc furnace (EAF) slags from two different steel companies have been studied. Both slags are produced during the melting of steel scrap in an EAF. The main difference within both is the cooling rate when obtaining. In one case, the melted slag is cooled rapidly by using water (EAF Slag 1) in a process that takes place in 3-4 hours and the other is cooled in open air during 2-3 days (EAF Slag 2). The impact of the different cooling rates has been determined in the experiments performed in this work.

The thermal and chemical stability was determined first by thermogravimetric analysis in the range of 200-1000°C. After that, small pebbles of both slags (around 10 grams each one) were put into alumina crucibles and then placed in a chamber furnace at 1000°C during 500 hours under air atmosphere. The samples of slag were structurally characterized before and after the tests by means of X-ray powder Diffraction (XRD) and superficially analyzed with Scanning Electron Microscopy (SEM) and Energy-dispersive X-ray (EDX) spectroscopy. The results are presented in Section 2.

In order to study the thermo-physical properties of both slags small pellets of 2 mm in thickness and 10 mm in diameter were prepared. The apparent density (ρ) was calculated at room temperature as a ratio of high precision

measured weight and volume of the samples. The heat capacity was determined with a Differential Scanning Calorimeter (DSC) and, the thermal conductivity (k) was indirectly calculated using the equation $k=\alpha\rho C_p$, where (α) is the thermal diffusivity obtained from Laser flash apparatus measurements. The results are presented in Section 3.

Finally, in order to determine the behavior of a TES device working in a packed-bed arrangement with EAF Slag as filler material and air as HTF under realistic conditions, Computational Fluid Dynamic (CFD) techniques has been used. In particular, the commercial CFD software ANSYS FLUENT[®] has been applied. The model and the simulation results are presented in Section 4, Section 5 is devoted to the conclusions.

Nomenclature

CFD	Computational Fluid Dynamics
C_p	Specific heat, J/gK
CSP	Concentrated solar power
D	Diameter, m
DSC	Differential Scanning Calorimeter
E	Energy, J
EAF	Electric arc furnace
EDX	Energy-dispersive X-ray
HTF	Heat transfer fluid
\dot{m}	Mass flow, kg/s
P	Power, W
p	Pressure, Pa
SEM	Scanning electron microscopy
TES	Thermal energy storage
XRD	X-ray diffraction
α	Thermal diffusivity, mm ² /s
k	Thermal conductivity, W/mK
ρ	Apparent density, kg/m ³
μ	Viscosity, kg/ms
v_∞	Velocity the fluid would have in the storage unit without any solid packed-bed, m/s

Subscripts

c	Charge
d	Discharge
f	Fluid
p	Particle

2. Thermal and chemical stability

The thermogravimetric analysis results obtained for both EAF slags are shown in the Fig. 1. In this figure, a complete heating-cooling cycle and an additional second heating curve for both materials are included. The continue line corresponds to the EAF Slag 1 and the discontinuous one to the EAF Slag 2.

From the figure, it can be observed that in both cases, during the first heating occurs a small gain in weight which is around 3% in the case of the EAF Slag 1 and around 5% in the case of the EAF Slag 2. However, no further mass change is observed in the subsequent cooling or heating runs. This transformation corresponds to the oxidation of some metallic (iron) parts and some metal oxides with low oxidation rates that are present in the slag. During the first heating process these elements are totally oxidized stabilizing the materials. As a consequence, it can be concluded that the transformed material after the first heating run is thermally stable, at least, up to 1000°C.

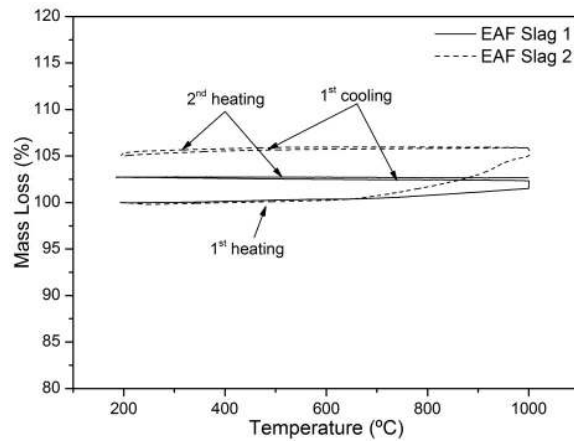


Fig. 1. Thermogravimetical analysis of both studied slags.

In Fig. 2 the XRD patterns of both studied slags are presented (on the top the EAF Slag 1 and on the bottom the EAF Slag 2) after being pre-treated in the furnace at 1000°C for 1h. In this figure, the circles correspond to the experimental data, the continuous line corresponds to the fitting profile obtained by Fullprof [16] and the vertical bars represent the Bragg peak positions of the detected phases. Table 1 shows the name, the chemical formulae and the PDF number of these phases. In addition, the identified phases are numerically labeled on the right side of the Fig. 2 and summarized in Table 1.

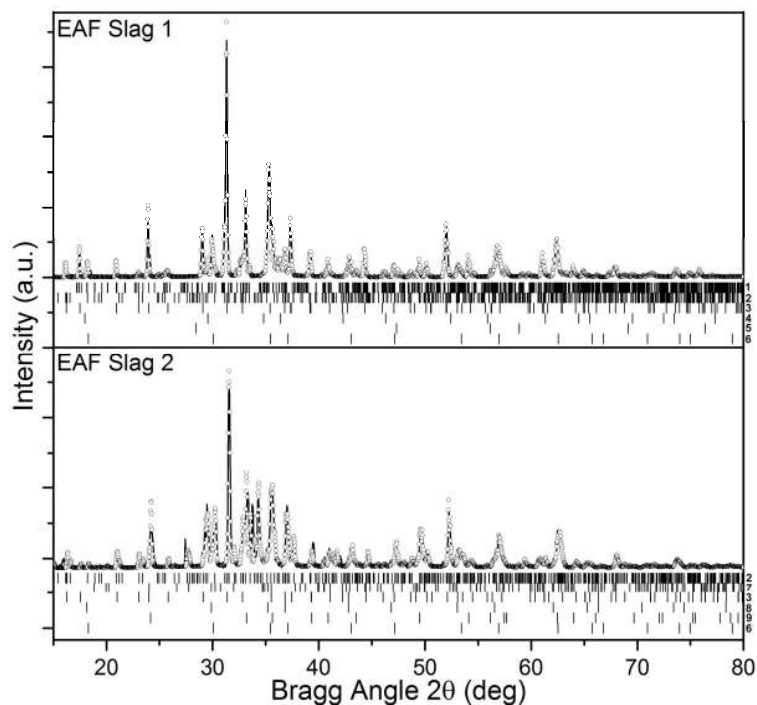


Fig. 2. XRD patterns of both pre-treated slags.

In Fig. 2 and Table 1 it can be observed that both slags are mainly composed of metal oxides forming different phases. The determination of these phases is an important factor in order to analyze the results of the corrosion test and also to detect any small transformation suffered by the tested slag.

Table 1. Phases detected in the XRD patterns.

Number	Name	Formulae	PDF Number
1	Calcium Aluminum Iron Oxide	$\text{Ca}_2\text{Al}_5\text{Fe}_7\text{O}_{20}$	01-056-0928
2	Bredigite	$\text{Ca}_{14}\text{Mg}_2(\text{SiO}_4)_8$	00-036-0399
3	Gehlenite	$\text{Ca}_2\text{Mg}_{0,25}\text{Al}_{1,5}\text{Si}_{1,25}\text{O}_7$	01-079-2422
4	Jacobsite	MnFe_2O_4	01-073-3820
5	Manganochromite	MnCr_2O_4	01-075-1614
6	Magnetite	$\text{Fe}_{2,897}\text{O}_4$	01-086-1343
7	Hedenbergite	$\text{Ca}(\text{Fe}_{0,821}\text{Al}_{0,179})(\text{SiAl}_{0,822}\text{Fe}_{0,178})\text{O}_6$	01-078-1546
8	Manganese Iron Oxide	$\text{Mn}_{0,43}\text{Fe}_{2,57}\text{O}_4$	01-089-2807
9	Hematite	Fe_2O_3	01-086-1343

Fig. 3 presents the XRD patterns of both slag types after the chemical compatibility tests performed with air at 1000°C during 500h. In this figure, the XRD patterns of both slags after the tests are presented. From the figure, it can be observed that there has not been any structural change neither in the experimental diffractograms nor in the detected phases. Furthermore, the values of the refined lattice parameters of detected phases before and after the compatibility tests are the same. Attending at these results, it can be concluded that there is no corrosion in the EAF Slags when working with air as HTF at temperatures up to 1000°C.

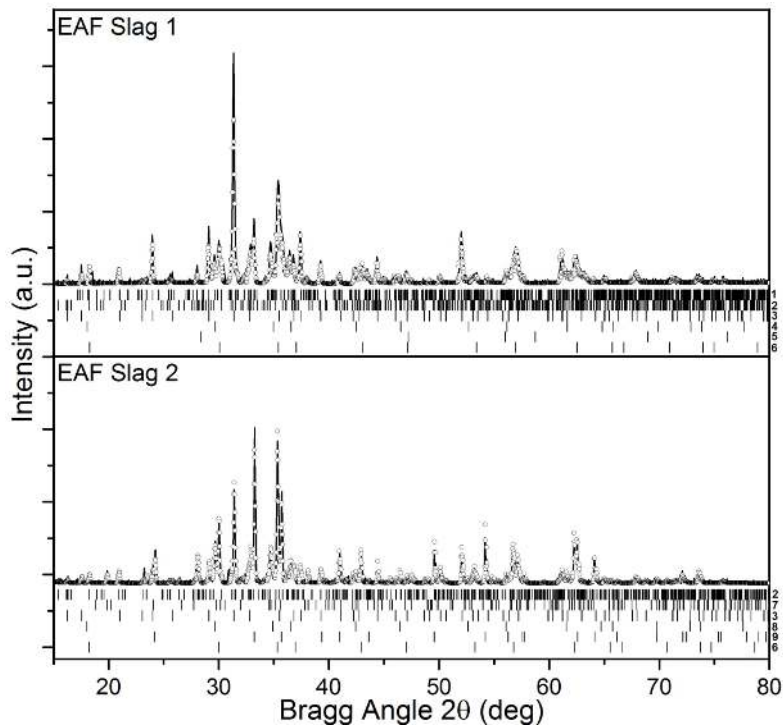


Fig. 3. XRD patterns of both tested slags.

3. Thermo-physical properties

In this part, the most relevant thermo-physical properties of the studied EAF slag have been analyzed. Table 2, shows the density values measured at room temperature, the heat capacity and the thermal conductivity at 350°C for these slags after being pre-treated as explained in the previous part.

It can be observed in this table, that the values obtained for the slags are similar to the other materials. As a consequence, it can be concluded that both EAF slags fulfill the standard requirements for a TES material working in a packed-bed arrangement. Furthermore, from the economic and environmental points of view, the slag looks more attractive than the other materials presented due to their expected lower price (waste material), their large availability and to save the primary resources.

Table 2. Thermo-physical properties of EAF Slag and different usual heat storage materials [7] [10] [17]

Property	EAF Slag 1	EAF Slag 2	Cofalit®	HT Concrete	Alumina (99.5%)
Density (kg/m ³)	3430	4110	3120	2750	3960
Specific Heat (J/kg K)	865	837	900	916	800
Thermal Conductivity (W/m K)	1.47	1.51	1.5-2.0	1.0	18.0

4. Modeling of the thermal storage

4.1. System description

The measured thermo-physical properties have shown the high potential of EAF slag to be used in packed-bed sensible heat storage applications. However, the operation of this heat storage solution needs a deep optimization effort in order to reach a successful management of the storage. In this work, a packed-storage arrangement based on EAF Slag 1 (since both studied slags show very similar properties) is proposed and computationally modeled as a function of the maximum outlet fluid temperature difference (tolerance, ΔT_{tol}) and cycling thermal behavior. In particular, $D_p = 1$ cm EAF slag pebble diameter has been studied in contact with air used as HTF. The operation parameters, potentially in agreement with new generation tower CSP plant requirements, are summarized in Table 3.

Table 3. Operation parameters.

Pebble diameter (cm)	1
Void fraction	0.37
Fluid flow rate (kg/s)	0.1
Hot fluid temperature (K)	1073
Cold fluid temperature (K)	873
Storage tank geometry	Cylindrical
Storage tank volume (m ³)	1
Storage tank aspect ratio (H/D)	2

According to the regular operation of this type of storage, during charge operation the hot air is supplied from the top of the tank whereas in discharge operation, the cold air is supplied from the bottom part. In both stages the fluid flow is assumed to be perfectly homogenous in the tank inlet/outlet.

Table 4. Operation modes based on the maximum allowed outlet temperature difference (ΔT_{tol}).

Operation Mode	End of charge ($x=L_{tank}$)	End of discharge ($x=0$)
1 $\Delta T_{tol}^1 = \pm 5K$	878	1068
2 $\Delta T_{tol}^2 = \pm 20K$	893	1053
3 $\Delta T_{tol}^{3,c} = +20K / \Delta T_{tol}^{3,d} = -5K$	893	1068

Based on the outlet temperature of the storage device on the charge and discharge process, three different operation modes have been modeled. The first one is associated to the usual requirements of an electricity production steam turbine, where the temperature tolerance allowed must be lower than $\Delta T_{tol}^1 = \pm 5K$. The second operation mode allows a higher inlet/outlet temperature tolerance of $\Delta T_{tol}^2 = \pm 20K$, appropriate for different heat demanding processes where the tolerance value is not as restrictive as in the turbine operation case. The third one establishes a mixed tolerance method for charge and discharge, $\Delta T_{tol}^{3,c} = +20K$ and $\Delta T_{tol}^{3,d} = -5K$ respectively. The

particular operation temperatures of each mode at the corresponding axial position of the storage tank are detailed in Table 4.

The obtained results have shown a strong impact on the thermal behavior of the storage system depending on the operation method.

4.2. Model description

In this work the commercial CFD ANSYS FLUENT® package has been used in order to model the thermal behavior of the packed-bed storage system. The fluid flow through a packed-bed has been modeled by using a porous media formulation based on Ergun equation, which is valid for a wide range of laminar and turbulent flow conditions. In this approach, no individual solid filler piece is modeled; the packed-bed is treated as a continuous porous material with a characteristic permeability, inertial loss and a void fraction assumed to a close random sphere packing arrangement ($\varepsilon=0.37$). Then, the heat transfer between the packed-bed and the fluid is essentially a transient problem where both phases are not in thermal equilibrium. For this reason, a two-phase model has been used. In this dual-cell approach, a solid domain is overlapped to the fluid zone with the associated porosity. Both zones are coupled only through heat transfer in a non-equilibrium thermal formulation with a constant heat transfer coefficient between the solid and fluid domains. For the calculation of this last parameter, the empirical Nusselt correlation suggested in [18], which is valid for $Re_p > 15$ (equation 1), has been selected (equation 2). In this approach, radiative heat transfer contribution has been neglected.

$$Nu = (2 + 1.1 Re_p^{0.6} Pr^{1/3}), \quad (1)$$

$$Re_p = \frac{v_\infty \rho_f D_p}{\mu_f}. \quad (2)$$

The modeling of packed-bed heat transfer phenomena involves complicated mechanisms and contributions of different natures. In order to include the most representative ones in the calculation in a simple approach, usually, an effective thermal conductivity value is calculated for both phases, k_f^{eff} and k_s^{eff} respectively. Several empirical and theoretical models have been developed in order to obtain these effective values in different fluid flow regimes (laminar and turbulent), packing arrangement (random, cubic etc.) and other physical parameters. In this work, the thermal conductivity of the solid and fluid phases have been determined following the model developed by Wakao and Kagueli [19], assuming isotropic behavior in the axial and radial directions.

The parameterization of the storage system has been performed in order to evaluate the governing magnitudes of the storage system according to the three different operation methods. The total input (charge) and stored energy (discharge), are calculated by evaluating the net inlet/outlet power introduced and extracted from the storage system during a charge/discharge run, as indicated in equation 3:

$$E_{\text{input / stored}} = \int_{t_c / t_d} (P_{\text{in}} - P_{\text{out}}) dt = \int_{t_c / t_d} \dot{m} c_p (T)(T_{\text{out}} - T_{\text{in}}) dt. \quad (3)$$

The total power loss through the lateral wall of the outer insulation layer in contact with atmospheric air is calculated according to the convective transfer equation 4 with an estimated $h = 7 \text{ W/m}^2\text{K}$ from the procedures in references [20, 21]:

$$P_{\text{wall}}^{\text{loss}} = \int_{\text{area}} h(T_{\text{ext}} - T_f) dA. \quad (4)$$

The pumping power due to the pressure drop introduced by the packed-bed has also been calculated according to equation 5:

$$E_{\text{pumping}} = \int_{t_c + t_d} \frac{\dot{m}}{\rho} \Delta p dt. \quad (5)$$

Overall, the total efficiency (η) of the system has been calculated for each operation method according to equation 6. It must be pointed out that the energy content of outlet fluid within the tolerance temperature range is considered as useful energy. In this case, the energy losses are restricted to the thermal losses through the lateral wall (already included in the input/output energy balance) and pumping losses ($E_{pumping}$):

$$\eta = \frac{E_{stored}}{E_{input} + E_{pumping}} \tag{6}$$

In all the simulated cases the initial conditions have been $v(x,r,t=0) = 0$ and $T(x,r,t=0) = T_f^{cold} = 873K$.

4.3. Results and discussion

The cyclic charge/discharge behavior of the air-slag packed-bed storage device for the three different operation modes is shown in Fig. 4. The curves show the temperature distribution along the axial position of the storage tank in the respective cases. In modes 2 and 3, after 10 operation charge/discharge runs, a stationary and reproducible behavior is attained while in mode 1 only a quasi-stationary state is accessible after the same number of cycles.

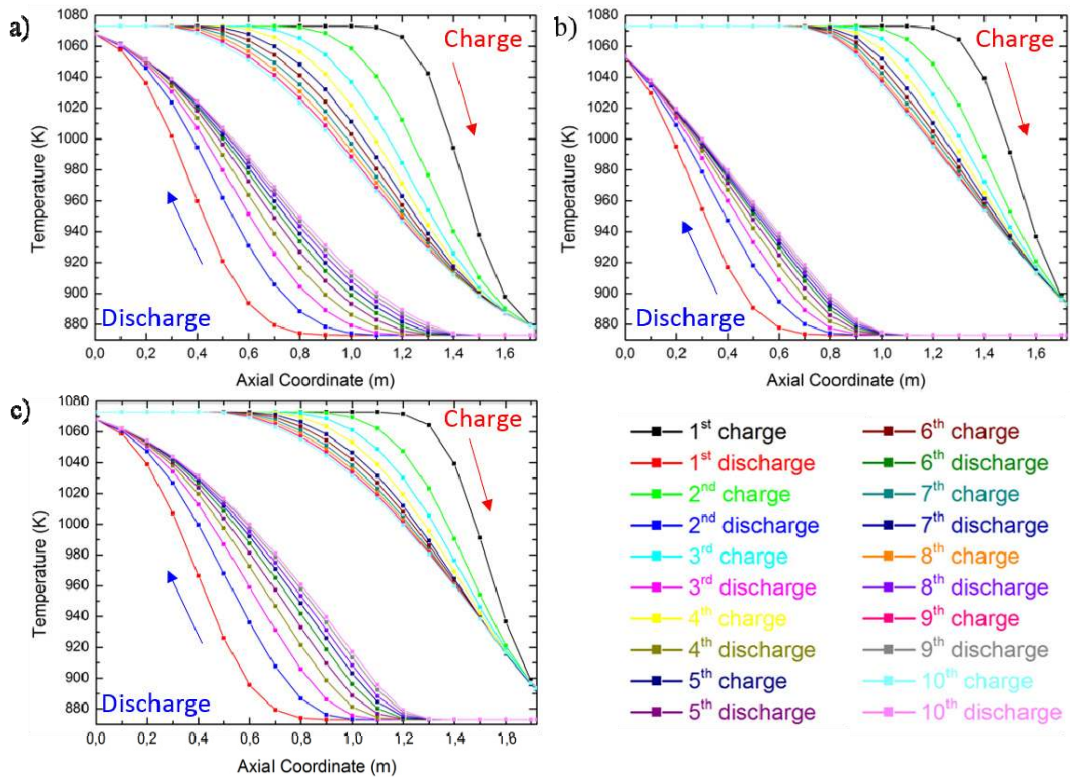


Fig. 4. Axial temperature distribution in the storage device for the operation modes 1 (a), 2 (b) and 3 (c). The curves show the transient behavior until the stationary state is attained on the 10th cycle.

As can be seen in Fig. 4a, the operation mode 1 implies a strong restriction for the modeled packed-bed storage, as the storage capacity is noticeably reduced after a certain number of working cycles. This limitation, derived from the small temperature tolerance value of $\Delta T_{tol}^1 = \pm 5K$ imposed by CSP steam turbine operation, avoids the extraction from the storage tank of a large fluid volume in the temperature gradient (thermocline) zone. As a consequence, after 10 cycles, the useful storage volume is reduced up to around the 25% of the total volume of the tank. In this case, considering the 10th cycle as a stationary state where all the extracted fluid with temperatures within the fixed tolerance is useful to produce energy, the overall efficiency is around 95% (see Table 5, value in

brackets) penalized by thermal losses through the tank wall (around 2% of the stored energy) and the pumping energy (around 1% of the storage). However, as can be seen in Fig. 4a, a stationary state is not feasible at least after ten cycles. For this reason, even if the total efficiency is very high, in order to maximize the stored energy, the transient operation of the storage device is more appropriate. In this operative methodology, a non-symmetric behavior will be obtained between the charge and discharge run, which reduces the overall efficiency depending on the performed cycles. However, the stored energy, as can be seen in (Table 5) is increased around 3 times if the operation is limited to the first cycle, or 2 times if it is extended to three cycles. All the quantitative results of this efficiency analysis are included in Table 5 for all the discussed operation modes.

Table 5. Energetic and efficiency analysis of the three evaluated packed-bed operation modes.

Parameter	$\Delta T_{tol}^1 = \pm 5K$			$\Delta T_{tol}^2 = \pm 20K$	$\Delta T_{tol}^{3,c} = +20K / \Delta T_{tol}^{3,d} = -5K$
	1 st Cycle	3 rd Cycle	10 th Cycle		
E_{input} (kWh)	95.5	51.2	26.1	58.4	40.2
E_{stored} (kWh)	70.3	46.7	25.0	56.4	38.8
Lateral Losses (kWh)	1.31	1.17	0.55	1.39	0.91
Pumping Losses (kWh)	0.93	0.55	0.29	0.66	0.46
Efficiency	0.58	0.70	0.80 (0.95)	0.95	0.95

However, this transient operation of the storage system implies the full discharge of the energy content in the packed-bed after the fixed number of charge/discharge runs, which will reduce the efficiency of this operation mode. In this work, the evaluation of this efficiency reduction has been carried out, as shown in Table 5. For the 1 cycle transient operation mode, the obtained efficiency is reduced around a 15%, whereas for the 3 cycle operation the reduction is higher, up to a 20%. This increasing energetic demand is related with the useful energy content of the storage, which decreases with cycling. As a consequence, the energetic cost of a full discharge increases, as the temperature gradient zone inside the packed-bed is larger. However, it should be noted that this extracted heat, not useful for energy production, could be valuable in other application within the CSP framework. In this work, in order to maintain an acceptable compromise between the efficiency and the total stored energy in the modeled air-steel slag packed-bed storage with an outlet temperature tolerance of $\Delta T_{tol}^1 = \pm 5K$, a transient operation of no more than 3 cycles is suggested.

On the other hand, if a larger outlet temperature tolerance is allowed for different applications, all the mentioned issues for transient operation can be removed. In this work, as an example, a larger tolerance of $\Delta T_{tol}^2 = \pm 20K$ has been selected for comparison (Fig. 4b). Although this value is not acceptable for the turbine operation, it could be appropriate for different applications within CSP technology and also for various renewable energy production fields, such as solar hydrogen production and others. In this operation method (2), the stationary operation of the packed-bed storage after 10 cycles can provide a large amount of energy, around 56kWh in our configuration. The thermal losses represent around 2.5% of the total storage whereas the pumping energy represents around 1%.

Taking into account the maximization of the stored energy with increasing outlet temperature tolerance values and the limitation imposed by the turbine operation, a mixed tolerance operation (3) could be also appropriate. In this case, one outlet temperature tolerance value is fixed for the charging process, which can be large as the output fluid is not used for power generation, and a tolerance appropriate for steam turbine operation is fixed during discharge of the storage. In our case, as can be seen in Fig. 4c, the charging tolerance has been fixed in $\Delta T_{tol}^{3,c} = +20K$ and the discharging one in $\Delta T_{tol}^{3,d} = -5K$. In this mixed operation mode the stored energy and efficiency is maximized maintaining the viability of the electricity production. The results show that a stationary operation is possible in this method after 10 charge/discharge runs. In this state, intermediate storage capacity and overall efficiency values between the operation modes (1) and (3).

5. Conclusions

A by-product from the steel industry is presented as a promising TES material for the next generation of CSP plants. The results have revealed that EAF slag is thermally stable at least, up to 1000°C. The compatibility analysis

with air as heat transfer fluid after 500h hours in direct contact has not revealed any corrosion issues. Moreover, thermo-physical properties measured in this work have shown appropriate values to be used as heat storage material.

Finally, a computational parametric study of a storage device working in air-slag packed-bed arrangement has been performed in the potential temperature range of new generation CSP plants. The impact of different operation modes based on the outlet temperature tolerances has been analyzed. The results show that depending on this parameter, a stationary state is not feasible in all the cases. This suggests the transient or mixed tolerance operation of the storage device in order to fulfill the power generation requirements and to maximize the storage capacity and efficiency.

Acknowledgements

This work has been supported by the Department of Economic Development and Competitiveness of the Basque government through the funding of the ETORTEK CIC Energigune-2013 research program.

The authors would like to thank Dr. Iñaki Loroño and the University of the Basque Country (UPV/EHU) for supporting the computational analysis within the frame of Euskoiker collaboration agreement, the companies ArcelorMittal and Productos Tubulares for kindly providing the samples of EAF slag and Naira Soguero for her collaboration in this work.

References

- [1] Kuravi S, Trahan J, Yogi Goswami D, Rahman MM, Stefanakos EK. Thermal energy storage technologies and systems for concentrating solar power plants. *Progress in Energy and Combustion Science* 2013; 39:285-319.
- [2] Gil A, Medrano M, Martorell I, Lázaro A, Dolado P, Zalba, Cabeza LF. State of the art on high temperature thermal energy storage for power generation. Part 1- concepts, materials and modellization. *Renewable and Sustainable Energy Reviews* 2010; 14:31–55.
- [3] Pitchumani R. SunShot Concentrating Solar Power Program. Thermochemical Energy Storage Workshop, January 8, 2013.
- [4] Solar thermal electricity. Strategic research agenda 2020-2025, ESTELA report December 2012.
- [5] Renewable Power Generation Costs in 2012: An Overview. IRENA report 2012.
- [6] Singh H, Saini RP, Saini JS. A review on packed bed solar energy storage systems. *Renewable and sustainable Energy Reviews* 2010; 14:1059-69
- [7] Khare S, Dell'Amico M, Knight C, McGarry S. Selection of materials for high temperature sensible energy storage. *Solar Energy Materials and Solar Cells* 2013; 115:114-122.
- [8] Py X, Calvet N, Olivès R, Meffre A, Echagut P, Bessada C, Veron, E, Ory S. Recycled Material for Sensible Heat Based Thermal Energy Storage to be Used in Concentrated Solar Thermal Power Plants. *Journal of Solar Energy Engineering* 2011; 133:3.
- [9] Faik A, Guillot S, Lambert J, Véron E, Ory S, Bessada C, Echegut P, Py X. Thermal storage material from inertised wastes: evolution of structural and radiative properties with temperature. *Solar Energy* 2010; 86 :139–46.
- [10] Calvet N, Meffre A, Olivès R, Guillot E, Py X, Bessada C, Echegut P. Matériau de stockage thermique par chaleur sensible pour centrales électro-solaires testé sous flux solaire concentré. *Congres Français de Thermique Le Touquet*, 25 au 28 mai 2010.
- [11] Calvet N, Gomez JC, Faik A, Roddatis VV, Meffre A, Glatzmaier GC, Doppiu S, Py X, Compatibility of a post-industrial ceramic with nitrate molten salts for use as filler material in a thermocline storage system. *Applied Energy* 2013; 109:387–93.
- [12] Meffre A, Py X, Olives R, Guillot S, Faik A, Bessada C, Echegut P, Michon U. High temperature thermal energy storage material from vitrified fly-ashes, *SolarPaces Proceedings* 2011.
- [13] Navarro ME, Martínez M, Gil A, Fernández AI, Cabeza LF, Olives R, Py X. Selection and characterization of recycled materials for sensible thermal energy storage. *Solar Energy Materials and Solar Cells* 2012; 107:131-135
- [14] Miró L, Navarro ME, Suresh P, Gil A, Fernández AI, Cabeza LF. Experimental characterization of a solid industrial by-product as material for high temperature sensible thermal energy storage (TES). *Applied Energy* 2014; 113:1261-1268.
- [15] European Slag Association, Position paper on the status of ferrous slag, April 2012.
- [16] Rodríguez-Carvajal, N. Recent advances in magnetic structure determination by neutron powder diffraction. *Physica B: Condensed Matter* 1993; 192: 55-59.
- [17] Laing D, Steinmann W-D, Tamme R, Richter C. Solid media thermal storage for parabolic trough power plants. *Solar Energy* 2006; 80: 1283-1289.
- [18] Alazmi B, Vafai K. Analysis of variants within the porous media transport models. *Journal Heat Transfer* 2000; 122:303-26.
- [19] Wakao N, Kagueli S. Heat and mass transfer in packed beds. Gordon and Braech, New York, 1982.
- [20] Zanganeh G, Pedretti A, Zavattoni S, Barbato M, Steinfeld A. Packed-bed thermal storage for concentrated solar power – Pilot-scale demonstration and industrial-scale design. *Solar Energy* 2012; 86: 3084–3098.
- [21] Incropera, F.P, Dewitt, D.P. *Fundamentos de transferencia de calor*. Pearson Prentice Hall, Mexico, 1999.